J. Biochem. 2020;168(3):285–294 doi:10.1093/jb/mvaa047

JB THE JOURNAL OF BIOCHEMISTRY

Biochemical properties of human full-length aryl hydrocarbon receptor (AhR)

Received February 29, 2020; accepted April 2, 2020; published online May 23, 2020

Seiya Uemura, Yasutomo Nakajima, Yuhki Yoshida, Moeko Furuya, Shun Matsutani, Shinya Kawate, Shun-ichi Ikeda, Noriko Tsuji, Ewa Grave, Hideki Wakui and Hideaki Itoh*

Department of Life Science, Graduate School and Faculty of Engineering Science, Akita University, Akita 010-8502, Japan

*Hideaki Itoh, Department of Life Science, Graduate School and Faculty of Engineering Science, Akita University, 1-1 Tegata Gakuen Town, Akita University, Akita 010-8502, Japan. Tel./Fax: +81-18-889-3041, email: itohh@gipc.akita-u.ac.jp

The aryl hydrocarbon receptor (AhR) is a very unstable protein. AhR binds to the molecular chaperone complex (HSP90-p23-XAP2) to maintain a stable structure in the cytoplasm. After binding to ligands, such as dioxin, AhR translocates from the cytoplasm to the nucleus with a molecular chaperone complex. The protein forms a heterodimer with Arnt after nuclear transfer, functions as a transcription factor by binding to a xenobiotic responsive element (XRE), and induces the cytochrome P450 1A1 (CYP1A1). Because of the unstable protein, expression of the full-length AhR in the *E. coli* expression system is very difficult. Many studies investigated AhR using AhR domains *in vitro*. We expressed and purified the human full-length AhR in *E. coli* expression system. Furthermore, specific antibodies were prepared. Purified full-length AhR could bind to ligand. In the presence of ligand, α-helix and random coil of AhR increased and *β*-sheet decreased on CD spectrum. Full-length AhR could bind to HSP90, XAP2 and p23 in the presence or absence of ligand. We now show the biochemical properties of full-length AhR.

Keywords: AhR; HSP; molecular chaperone; secondary structure.

Abbreviations: 3-MC, 3-methylcholanthrene; AhR, aryl hydrocarbon receptor; Arnt, aryl hydrocarbon receptor nuclear translocator; bHLH, basic helix-loop-helix; CYP1A1, cytochrome P450 1A1; DTT, dithiothreitol; FCS, foetal calf serum; HSP90, 90-kDa of heat shock protein; IPTG, isopropyl-1-thio-*β*-d-galactopyranoside; NES, nuclear export signal; NLS, nuclear localization signal; PAH, polycyclic aromatic hydrocarbon compound; PAS, Per-Arnt-Sim; SDS–PAG, sodium dodecyl sulphate polyacrylamide gel electrophoresis; TAD, transcriptional activation domain; TCDD, 2,3,7,8-tetrachlorodibenzo-*p*-dioxin; XAP2, hepatitis B virus X-associated protein 2; XRE, xenobiotic responsive element; *β* -NF, *β*-naphthoflavone.

The aryl hydrocarbon receptor (AhR) is a nuclear receptor and plays role as a ligand-activated transcription factor (*1*, *2*). Human AhR is a protein consisting of 848 amino acids and is composed of several functional domains. A basic helix-loop-helix (bHLH) domain is present in the N-terminal region of the protein. The domain is a dimerization domain and it possesses a nuclear localization signal (NLS) and nuclear export signal (NES). The Per-Arnt-Sim (PAS) domain is present in the middle region of AhR and constituted by PAS-A and PAS-B domain. The PAS-A domain is involved in dimer formation, and the PAS-B domain is ligand-binding site (*3*–*5*). The transcriptional activation domain (TAD) is near the C-terminal region of AhR and contains glutamine (Q) rich site (*6*, *7*).

AhR binds many polycyclic aromatic hydrocarbon compounds (PAH) as ligands and plays an important role in xenobiotic response to food or environmental substances. The ligands are 2,3,7,8-tetrachlorodibenzo-*p*-dioxin (TCDD), 3-methylcholanthrene (3-MC), β-naphthoflavone (β-NF) and the like (*8*). In the absence of ligands, AhR exists in the cytoplasm in a complex with molecular chaperones HSP90, hepatitis B virus X-associated protein 2 (XAP2), and co-chaperone p23 (*9*–*13*). HSP90 is the most expressed protein in cytoplasm of eukaryotic cells, and it regulates over 300 client proteins (*14*, *15*). HSP90 binds to bHLH- and PAS-B domains (*16*–*18*).

After the ligand binds to the AhR, the AhR translocates to the nucleus with the molecular chaperone complex. After translocation to the nucleus, AhR dissociates from the molecular chaperone complex and forms a heterodimer with the aryl hydrocarbon receptor nuclear translocator (ARNT) via the bHLH and PAS-A domains. The bHLH domain of this heterodimer binds to the xenobiotic responsive element (XRE) to induce the toxin-metabolizing enzyme cytochrome P450 1A1 (CYP1A1) (*19*, *20*). However, dioxins such as TCDD accumulated in the body without being metabolized (*21*). For the induction of eukaryotic transcription factors, high expression systems using *E. coli* may not work. It is very difficult to express recombinant full-length AhR because the Q-rich TAD of AhR is toxic to *E. coli*. Few reports have been reported on the expression of full-length AhR in

baculovirus , but the expression of full-length AhR in *E. coli* has not been reported (*22*, *23*). Therefore, we investigated the activation mechanism of AhR using the AhR functional domain (*16–18*). In this study, we attempted to express full-length AhR and investigated the activation mechanism using full-length AhR instead of the AhR domain.

Materials and Methods

Materials

Isopropyl-1-thio-β-$_D$-galactopyranoside (IPTG) was purchased from Nakarai Tesque (Kyoto, Japan). 3-Methylcolanthrene (3-MC) was purchased from Sigma-Aldrich Japan. β-naphthoflavone (β-NF) was purchased from Tokyo Chemical Industry. An anti-AhR antibody (sc-5579) was purchased from Santa Cruz Biotechnology. An Alexa Fluor 488 conjugated anti-mouse antibody and Alexa Fluor 546 conjugated anti-rabbit antibody were purchased from Invitrogen.

Cell culture

Cervical tumor-derived HeLa cells were obtained from ATCC. Cells were cultured in plastic dishes (Greiner, Germany) containing DMEM medium (Sigma-Aldrich Japan) supplemented with 5% foetal bovine serum (FBS) at 37°C under 5% CO_2 and 95% humidity.

Plasmid constructions

The total RNA was isolated from the HeLa cells using the RNeasy Mini Kit (Qiagen, Valencia, CA). The amount and purity of the total RNA was estimated by spectrophotometric analysis at A260 and A280. The RNA quality was determined by agarose gel electrophoresis following ethidium bromide staining. Aliquots of the total RNA were diluted in diethylpyrocarbonated (DEPC)-treated water and stored at −80°C. RNA (4 μg) was used to synthesize the first-strand complementary DNA (cDNA) with Super Script III First-Strand (Invitrogen) under the following general conditions: denaturation at 94°C for 15 s, annealing at 55°C for 30 s and extension at 68°C for 30 s for up to 40 cycles using an iCycler (BioRad). The cDNAs were PCR-amplified by iCycler (BioRad) with the primers of AhR. The full-length AhR was amplified by PCR (iCycler, BioRad) using the forward primer 5′-GTCGACATGAACAGCAG CAGCGCCAAC-3′ and reverse primer 5′-GCGGCCGCTTACAG GAATCCACTGGATGTCAAA-3′. The resulting PCR products were inserted into the SalI/NotI sites of the pGEX-5X-3 vector (Takara Bio, Japan). Factor Xa Protease site of pGEX-5X-3 was replaced with PreScission Protease site/human rhinovirus protease 3C (HRV3C) sequence (LEVLFQGP) by PrimeSTAR Mutagenesis Basal Kit (Takara Bio, Japan). This replacement was achieved by performing three PCR reactions in sequence using the following primer pairs: First time; forward primer 5′-AACCTTTATTTTCAA GGTCGTGGGATCCCCAGG-3′ and reverse primer 5′-TTGAAA ATAAAGGTTTTCGATCAGATCCGATTT-3′, second time; forward primer 5′-TCCTTGAAGTCCTTTTTCAAGGTCGTGGGA TCC-3′ and reverse primer 5′-AAAGGACTTCAAGGATCAGA TCCGATTTTGGAG-3′ and third time; forward primer 5′-CA AGGTCCCGGGATCCCCAGGAATTCC-3′ and reverse primer 5′-GATCCCGGGACCTTGAAAAAGGACTT-3′. The constructs were confirmed by DNA sequencing (PRISM 3100, ABI).

Recombinant protein expression and purification

The following indicates a method that GST-AhR was purified from the insoluble fraction for antibody production. The GST-tagged AhR was expressed from the expression vector pGEX-5X-3 in an *E. coli* OverExpress C41 (DE3) pLysS competent cell (Lucigen). The cells were grown at 37°C, 250 rpm in LB BROTH medium supplemented with 100 μg/ml ampicillin until the OD_{600} reached 0.6. The cells were then induced by the addition of 1.0 mM IPTG, and the culture medium was incubated at 37°C, 250 rpm for an additional 3 h. The cells were harvested by centrifugation at 4°C, 13,000 rpm for 15 min, and cell pellets were suspended in 10 mM Tris–HCl buffer (pH 7.4). The cells were sonicated, centrifuged at 4°C, 13,000 rpm for 15 min and the formed pellets were collected. The collected pellets were suspended in buffer (1 M arginine, 10 mM Tris–HCl buffer (pH 7.4)), then applied to desalting column, Bio-Gel P-6DG Gel (BioRad) to remove the arginine. After desalting, GST-AhR was digested by PreScission Protease (GE Healthcare) to remove GST tag. Desalted solution that contained GST-AhR was digested by PreScission Protease in digestion buffer containing 50 mM Tris–HCl buffer (pH 7.0), 150 mM NaCl, 1 mM EDTA and 1 mM dithiothreitol (DTT). PreScission Protease was added in 90 units per 1 ml *E. coli* disruption solution. The digestion reaction was incubated at 4°C, 5 rpm for 16 h. After digestion, analysed by SDS-PAGE (7%) and eluted AhR from SDS-PAGE gel by MODEL BE-883 (BIO CRAFT).

The following indicates a method that purified the GST-AhR from soluble fraction for protein analysis. The GST-tagged AhR was expressed from the expression vector pGEX-5X-3 in an *E. coli* OverExpress C41 (DE3) pLysS competent cell (Lucigen). The cells were grown at 37°C, 250 rpm in LB BROTH medium supplemented with 100 μg/ml ampicillin until the OD_{600} reached 0.5. The culture medium was cooled for 30 min to 10°C. The cells were then induced by the addition of 1.0 mM IPTG and incubated at 10°C, 250 rpm for an additional 48 h. The cells were harvested by centrifugation at 4°C, 13,000 rpm for 15 min, and cell pellets were suspended in 10 mM Tris–HCl buffer (pH 7.4). The cells were sonicated for two cycles, centrifuged at 4°C, 15,000 rpm for 15 min, then the supernatants were collected. Proteins were applied to the Q-Sepharose column (GE Healthcare), then the pass-through fraction was collected. Pass-through fraction was applied to the Glutathione Sepharose 4B column (GE Healthcare), washed with 0.5 M NaCl in 10 mM Tris–HCl buffer (pH 7.4). After washing proteins were eluted with 20 mM glutathione in 50 mM Tris–HCl buffer (pH 8.0). Finally, the eluted proteins were concentrated by ultrafiltration. After ultrafiltration, GST-AhR was digested by PreScission Protease (GE Healthcare) to remove GST tag. Purified GST-AhR was digested by PreScission Protease in digestion buffer containing 50 mM Tris–HCl buffer (pH 7.0), 150 mM NaCl, 1 mM EDTA and 1 mM dithiothreitol (DTT). PreScission protease was added in 50 units per 250 μg purified GST-AhR. The digestion reaction was incubated at 4°C, 5 rpm for 16 h. After digestion, applied to the Glutathione Sepharose 4B column (GE Healthcare), then the pass-through fraction was collected.

The HSP90, XAP2 and p23 were expressed and purified in previously reported (*20*, *21*).

Antibody production

An anti-AhR antibody was produced by intramuscular injection into a rabbit of AhR that was eluted from SDS-PAGE gel emulsified in complete Freund's adjuvant. Booster shots were given three times in the same manner as the original injection at 2-week intervals. The rabbit was bled 10 days after the last injection. Original injection was 200 μl of AhR, Booster shots were 600 μl of AhR. An anti-HSP90, anti-p23 and anti-XAP2 antibody were produced by intramuscular injection into a rabbit of 1 mg of the purified each protein emulsified in complete Freund's adjuvant. Booster shots were given three times in the same manner as the original injection at 2-week intervals. The rabbit was bled 10 days after the last injection.

The protocols for animal experimentation described in this article were previously approved by the Animal Research Committee, Akita University School of Medicine; the 'Guidelines for Animal Experimentation' of the University were completely adhered to in all subsequent animal experiments.

β-naphthoflavone affinity chromatography

β-NF-Sepharose was prepared using β-NF and Epoxy-activated Sepharose 6B (GE Healthcare) according to the manufacturer's instructions. The purified GST-AhR was digested using PreScission Protease (GE Healthcare) according to the manufacturer's instructions. The digested samples and undigested samples were added to β-NF-Sepharose or Mock (without β-NF)-Sepharose equilibrated with 50 mM HEPES-KOH buffer (pH 7.4) and incubated with gentle rotation using a rotator for 1 h at 4°C. After washing with the same buffer three times, the bound proteins were eluted from the resin by adding 5 mM β-NF. The eluted proteins were separated by SDS–PAGE and detected by immunoblotting using an anti-AhR antibody.

Circular dichroism

Circular dichroism was performed using a Jasco J-720 spectropolarimeter (Jasco). About 1/1000 amount of DMSO or 5 mM 3-MC in DMSO was added to 1.5 μM AhR in 10 mM Tris–HCl buffer (pH 7.4). CD spectra were collected using instrumental parameters: $190 < \lambda < 250$ nm, 0.2 nm step size, 100 nm/min scan rate, 1.0 s integration time, 2.0 nm bandwidth, in a 0.1 cm cell, with six total scans averaged. Secondary structure was predicted using J-720 for Windows protein secondary structure analysis (Jasco, Japan).

Molecular modelling

Molecular modelling was performed using a MF myPresto v2.1 (FiatLux). The structural data of HIF-2α were obtained from Protein Data Bank (PDB ID: 3H82) (*24*). 3H82 shows a structure of the heterodimer of HIF-2α and ARNT C-terminal PAS domains. Docking simulation with ligand was performed using the structure of PAS-B of HIF-2α extracted from 3H82. Topology data and grid potential were set up using default parameters. The calculation method in the Sievgene docking simulation was performed by Precise.

Prediction of secondary structure

Secondary structure prediction was performed using PredictProtein and PROFphd-Secondary Structure, Solvent Accessibility and Transmembrane Helices Prediction software. The sequence data of AhR was obtained from Human Protein Reference Database (HPRD ID: 02596).

Co-immunoprecipitation

For the co-IP, 2.5 μM GST-AhR, HSP90, XAP2 and p23 were added to 250 μl buffer A (0.1 M KCl/10 mM $MgCl_2$/20 mM Na_2MoO_4/0.6 M NaCl/5% Glycerol/0.1% NP-40 in 25 mM HEPES-KOH buffer (pH 7.4)). The total volume of the sample was 500 μl by adding buffer B (5% Glycerol/0.1% NP-40 in 25 mM HEPES-KOH buffer (pH 7.4)). Anti-AhR antibody or preimmune rabbit IgG was added to these samples and incubated using a rotator with gentle rotation at 4°C for 16 h. The samples were loaded onto 50 μl Protein A Sepharose (GE Healthcare, Japan) which were prewashed with buffer C (50 mM KCl/5 mM $MgCl_2$/10 mM Na_2MoO_4/0.3 M NaCl/5% Glycerol/0.1% NP-40 in 25 mM HEPES-KOH buffer (pH 7.4)) twice and incubated using a rotator with gentle rotation at 4°C for 1 h. After incubation, the samples were centrifuged at 4°C, 5,000 rpm for 10 s to remove the supernatant. The beads were washed three times with buffer C and eluted by boiling at 100°C for 5 min in SDS sample buffer. The bound proteins were separated by SDS-PAGE and visualized by immunoblotting using an anti-HSP90, anti-XAP2 and anti-p23 antibody.

Results

Expression and purification of GST-AhR

In the current study, to express and purify the human full-length AhR, we constructed the pGEX-5X-3-AhR expression vector as the GST-AhR fusion protein (Fig. 1). We tried to express the GST-AhR using *E. coli* BL21 (DE3) competent cell. Although we induced the fusion protein by IPTG, we could not detect the GST-AhR in the soluble fraction on SDS-PAGE (Fig. 2A). We then tried to express the protein using the *E. coli* OverExpress C41 (DE3) pLysS competent cell. After the addition of IPTG, the cells were incubated at 37°C for 3 h. Although the expression level of AhR in the insoluble fraction was increased, the protein was not expressed in the soluble fraction. Therefore, we attempted to express AhR by low-temperature culture at 10°C. As shown in Fig. 2B, GST-AhR was induced mainly in soluble fraction. The induced protein was cross-reacted to the anti-human AhR antibody. In the present study, we confirmed the protein as AhR with this antibody. After the addition of IPTG, the cell was incubated at 10°C for 24 or 48 h. The GST-AhR protein was expressed both in the soluble and insoluble fractions (Fig. 2C). In the expression analysis of GST-AhR, the expression efficiency of the fusion protein in the soluble and insoluble fractions were the maximum at 1.0 mM IPTG and incubation time of 48 h.

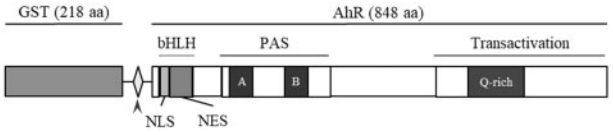

Fig. 1. Schematic diagram of the GST-AhR fusion protein. The arrow head indicates PreScission digestion site. bHLH and PAS indicate basic helix-loop-helix and PER-ARNT-SIM domain, respectively. NLS and NES indicate nuclear localization signal and nuclear export signal, respectively.

We first tried purification of GST-AhR from the insoluble fraction. The insoluble proteins were dissolved in 1.0 M arginine as described in the Materials and Methods section. After removal of arginine, GST-AhR was digested using a PreScission protease. As shown in Fig. 2D, AhR was cut from GST-AhR (lane 3). We cut the AhR proteins band from the SDS-polyacrylamide gels, and proteins were eluted from the gel (Fig. 2D). We electrophoretically purified the full-length AhR. We next tried to make an antibody against the full-length AhR. As shown in Fig. 2E, the antibody cross-reacted to GST-AhR and AhR. The antibody was highly specific against AhR.

Purification and characterization of full-length human AhR

We tried to purify the AhR from the soluble fraction. The purification of GST-AhR was done using a Q-Sepharose column and Glutathione Sepharose 4B column. The supernatant of *E. coli* was applied onto a Q-Sepharose column, the pass-through fraction was collected and applied onto a Glutathione Sepharose 4B column. After washing the column, GST-AhR was eluted from the column using 20 mM Glutathione in 50 mM Tris–HCl buffer (pH 8.0). We could detect the GST-AhR as a major protein band on SDS-PAGE (Fig. 3A, lane 1). The purified GST-AhR was digested using PreScission protease (Fig. 3A, lane 2). As shown in Fig. 3B, lane 1, there are three proteins band of AhR (97 kDa), PreScission protease (46 kDa) and GST (26 kDa). We excluded GST and the PreScission protease using Glutathione Sepharose 4B. Finally, we could purify the full-length human AhR as a native protein (Fig. 3B, lane 2). We investigated binding ability of the purified AhR to the ligand. Although no protein binds to the mock resin, the purified AhR were applied to β-NF resin and eluted from the resin by adding of 5 mM β-NF. We could detect β-NF-bound AhR on immunoblot (Fig. 3C). The purified AhR possesses ligand-binding ability. We investigated the secondary structure of purified AhR using CD spectrum. In the presence of ligand, the secondary structure of AhR has been changed (Fig. 3D). Decrease of β-sheet (217 nm) and increase α-helix (206 nm) and random structure (190 nm) as the

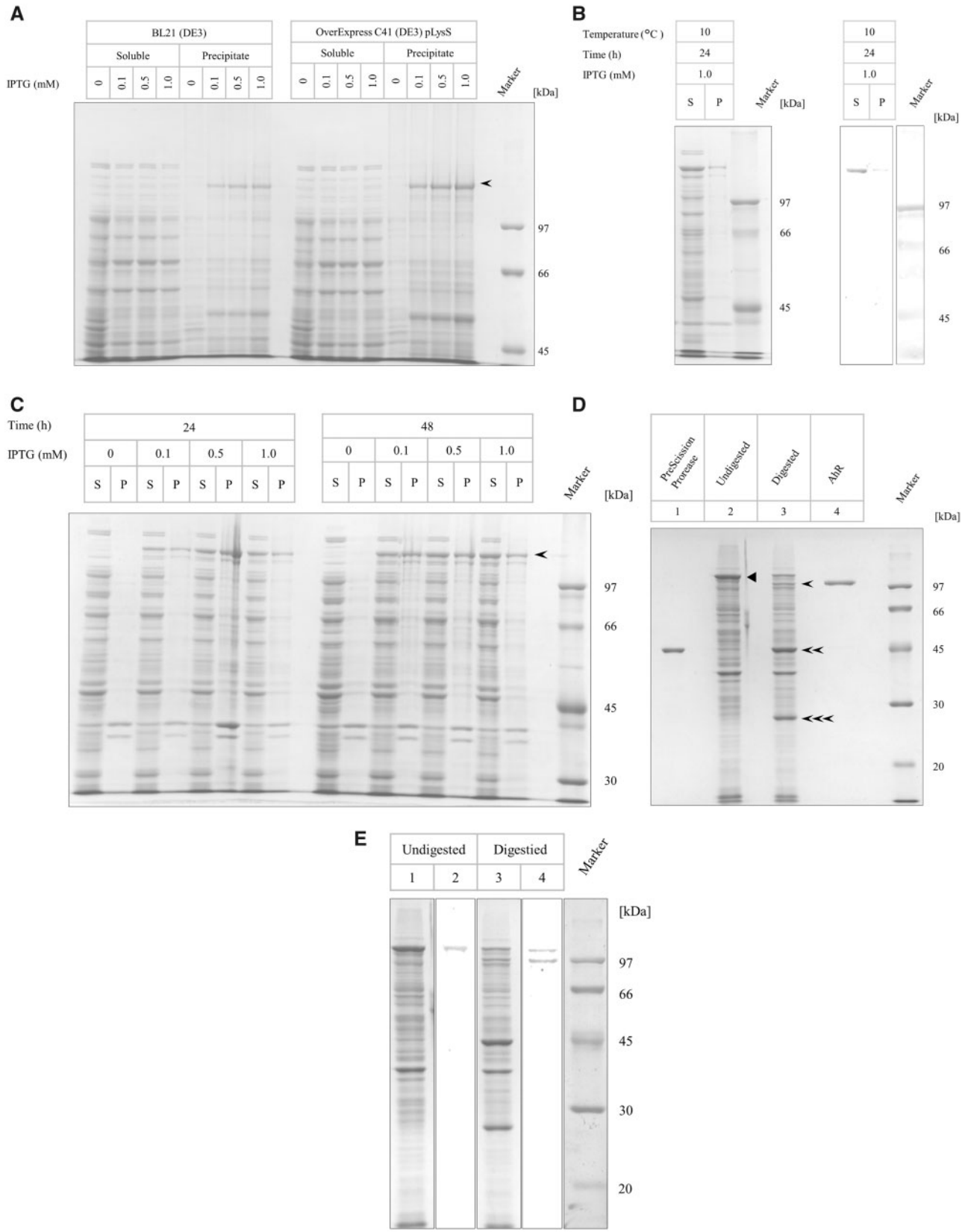

Fig. 2. Induction and analysis of an antibody against full-length AhR. (**A**) Plasmid pGEX-5X-3-AhR was transformed into BL21 (DE3) and OverExpress C41 (DE3) pLysS competent cell. Protein expression was induced by 0, 0.1, 0.5, 1.0 mM IPTG and incubation for 3 h at 37°C. After expression, the cells were harvested by centrifugation at 4°C, 15,000 rpm for 15 min, and cell pellets were suspended in 10 mM Tris–HCl buffer (pH 7.4). The cells were sonicated, centrifuged at 4°C, 15,000 rpm for 15 min and soluble fraction (soluble) and insoluble fraction (precipitate) were collected. Proteins were separated by SDS-PAGE (7% gel) and stained with CBB. Left column shows expression of GST-AhR in BL21 (DE3), and right column shows in OverExpress C41 (DE3) pLysS. The arrow shows GST-AhR. (**B**) pGEX-5X-3-AhR was transformed into OverExpress C41 (DE3) pLysS competent cells. The protein was induced by incubation for 24 h at 10°C after the addition

(continued)

negative cotton effect. Changes in secondary structure were shown in Table I.

Molecular modelling of AhR

The interaction between AhR and ligand was verified using a molecular model. However, 3D structure of AhR has not been clarified. We used the PAS-B structure of HIF-2α (hypoxia-inducible factor-2α) as a template to predict the structure of AhR. Hypoxia-inducible factor is protein that is induced when the supply of oxygen to cells falls short (*25*). HIF2a belongs to the same bHLH-PAS family as AhR, and functions as a transcription factor (*26*). HIF2a has 51% amino acid homology to AhR and is used as a template structure for AhR (*27*). The PAS-B structure of HIF-2α contains two α-helix, five β-sheets and random structure (Fig. 4A). On the contrary, we speculate the secondary structure of human AhR PAS-B domain using PredictProtein using PROFphd-Secondary Structure, Solvent Accessibility and Transmembrane Helices Prediction software. As shown in Fig. 4B, there was three α-helix, and four β-sheets, and random structure. Secondary structure type in the PAS-B domain of human AhR were 23.94% H (α-helix), 23.94% E (β-sheets) and 52.11% L (irregular structure). The PAS-B structure of human AhR was almost the same as the PAS-B structure of HIF-2α. The structure of AhR with TCDD, β-NF and 3-MC ligands were shown in Fig. 4C. All these ligands may be able to bind near β-sheets of the PAS domain (Fig. 4A). If the ligand binds well to the receptor, the docking score will show a negative number, with higher negative numbers meaning better docking. The docking score of these ligands to AhR were shown in Table II. The docking scores of TCDD, β-NF and 3-MC showed the negative number. We used reserpine and methotrexate as negative control molecule (Supplementary Fig. S1A). Both molecules penetrated the PAS-B domain (Supplementary Fig. S1B), and the binding score showed a large positive number (Table II).

Full-length AhR binds to the chaperone complex

We purified HSP90, XAP2 and p23 (Fig. 5A) and investigated the AhR-chaperone complex by an immunoprecipitation. Immunoprecipitation was performed using an antibody against AHR, and proteins were detected on the immunoblot using an antibody against HSP90, an antibody against XAP2 and an antibody against p23. In the absence or a presence of ligand, HSP90, XAP2 and p23 were detected (Fig. 5B).

Discussion

The expression and purification of the full-length AhR using the *baculovirus* expression system has been reported before (*18*, *19*). There are no reports for the purification of full-length AhR using the *E. coli* expression system. We tried to express and purify the full-length AhR using some *E. coli* expression vector systems or some *E. coli* competent cells, such as the ArcticExpress competent cells, ArcticExpress (DE3) competent cells, Origami B (DE3) competent cells and Rosseta B (DE3) competent cells. However, little to negligible AhR was expressed in insoluble fraction. AhR possesses the Q-rich domain in the C-terminal transactivation domain (Fig. 1). The Q-rich domain is toxic for *E. coli*, so AhR is difficult to express in the *E. coli* expression system. OverExpress C41 (DE3) pLysS holds chloramphenicol-resistant plasmid encoding T7 lysozyme which is a natural inhibitor of the T7 RNA polymerase. The cell including pLysS produces a little T7 lysozyme. This strain is used to stabilize a recombinant encoding particularly toxic protein.

We tried to express the full-length AhR using the OverExpress competent cell. We constructed and purified the full-length AhR as GST-AhR using the competent cells. The fusion protein was expressed both in the soluble and insoluble fractions. The competent cells were effective to express toxic proteins in soluble fraction. We finally purified human full-length AhR. Then, we investigated ligand-binding ability of the purified protein. Epoxy-activated Sepharose 6B can immobilize ligand containing C=O, N=N and C=C bonds. In the AhR ligands, such as TCDD, 3-MC and β-NF, only β-NF contains C=O bond. We prepared β-NF affinity resin using epoxy-activated Sepharose 6B. Although no protein binds to epoxy-activated Sepharose 6B (mock resin), the purified AhR from the soluble fraction could bind to the β-NF affinity resin (Fig. 3C). These results suggested that purified full-length AhR from soluble fraction possesses ligand-binding ability.

Fig. 2. Continued
of 1.0 mM IPTG. After expression, *E. coli* was collected by centrifugation at 4°C, 15,000 rpm for 15 min and the precipitate was suspended in 10 mM Tris–HCl buffer (pH 7.4). The *E. coli* was sonicated and centrifuged 15,000 rpm for 15 min at 4°C to separate into soluble and insoluble fractions. S and P indicate a soluble and insoluble fraction, respectively. Proteins were analysed by SDS-PAGE (7%). Immunoblot was performed by incubation for 24 h at 10°C using an anti-AhR antibody (sc-5579). (**C**) Plasmid pGEX-5X-3-AhR was transformed into OverExpress C41 (DE3) pLysS competent cell. Protein expression was induced by 0, 0.1, 0.5, 1.0 mM IPTG and incubation for 24 or 48 h at 10°C. After expression, the cells were harvested by centrifugation at 4°C, 15,000 rpm for 15 min, and cell pellets were suspended in 10 mM Tris–HCl buffer (pH 7.4). The cells were sonicated, centrifuged at 4°C, 15,000 rpm for 15 min and soluble fraction (S) and insoluble fraction (p: precipitate) were collected. Proteins were separated by SDS-PAGE (9% gel) and stained with CBB. Left column shows expression of GST-AhR in OverExpress C41 (DE3) pLysS for 24 h, and right column shows OverExpress C41 (DE3) pLysS for 48 h. The arrow shows GST-AhR. (**D**) Electrophoretical purification of AhR. Induced GST-AhR in the precipitate was dissolved in 1 M arginine and digested using PreScission protease. The digested proteins were analysed by SDS-PAGE (12% gel). The triangle in lane 2 indicates GST-AhR. The single arrow head, double arrow heads and triple arrow heads in lane 3 indicate digested AhR, PreScission protease and GST, respectively. Digested the AhR-protein band was cut and the AhR was eluted from the gels. Lane 4, the electrophoretically purified AhR. (**E**) Specificity of antibody. Undigested or digested GST-AhR by PreScission protease were analysed by SDS-PAGE (12% gel, lanes 1 and 3) followed by immunoblotting with an anti-AhR antibody (lanes 2 and 4).

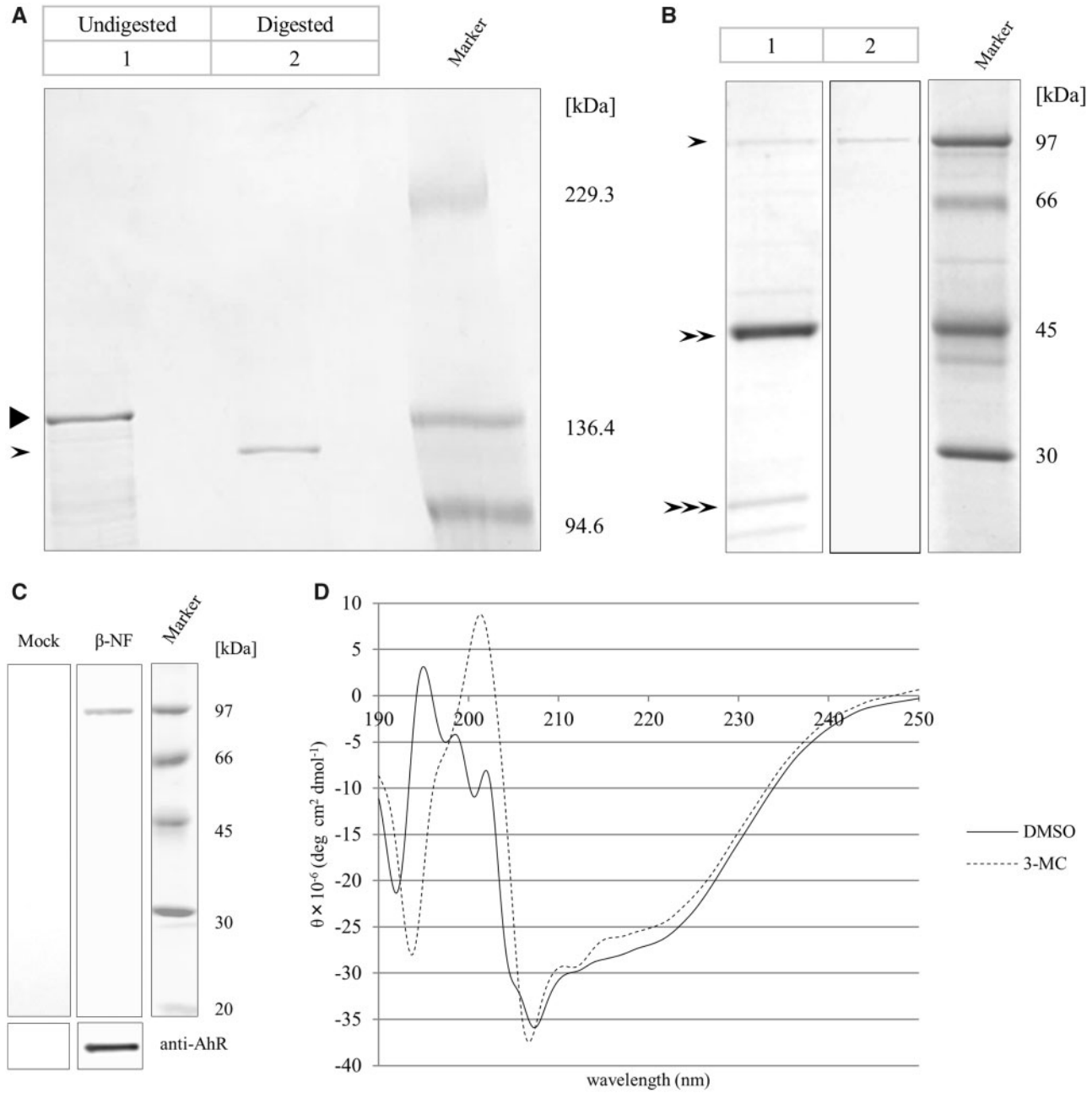

Fig. 3. Purification and analysis of ligand binding of AhR. (**A**) Purification of the GST-AhR fusion protein. The GST-AhR, induced in the soluble fraction, was applied onto Q-Sepharose and Glutathione Sepharose 4B column, and eluted with 20 mM Glutathione. Eluted protein was digested using PreScission protease. Undigested and digested proteins were analysed by SDS-PAGE (5% gel). Undigested GST-AhR in lane 1 indicate triangle. Digested AhR in lane 2 indicate arrow head. (**B**) Purification of full-length native AhR. Digested AhR, PreScission protease and GST in lane 1 were applied onto Glutathione Sepharose 4B. Lane 2 shows AhR which removed PreScission protease and GST. Single arrow head indicates full-length AhR, double arrow heads indicate PreScission protease, and triple arrow heads indicate GST. Proteins were analysed by SDS-PAGE (11% gel). (**C**) Ligand-binding activity of AhR. Purified AhR was added to the β-naphthoflavone (β-NF) affinity resin or mock resin (epoxy-activated Sepharose 6B) and eluted with 5 mM β-NF. The eluted proteins were analysed by SDS-PAGE followed by immunoblotting with an anti-AhR antibody. (**D**) Circular dichroism spectrometry of AhR. The circular dichroism spectrum of AhR in the presence or absence of 3-MC was measured. The solid line indicates the absence of 3-MC (DMSO), and the broken line indicates presence of 3-MC. The graph shows $\theta \times 10^{-6}$ at wavelengths from 190 to 250 nm.

Table I. Secondary structure of prediction of AhR

	DMSO	3-MC
Helix	16.0	24.0
Beta	30.1	4.3
Turn	20.8	35.0
Random	33.1	36.7

We also analyse the conformational changes of AhR in the presence or absence of ligands on CD spectrum. In the absence of ligand, the CD spectrum pattern of AhR showed basic protein secondary structure, such as α-helix, β-sheet and random coil. On the contrary, increase of α-helix and random coil and decrease of β-sheet in the presence of ligand. We could

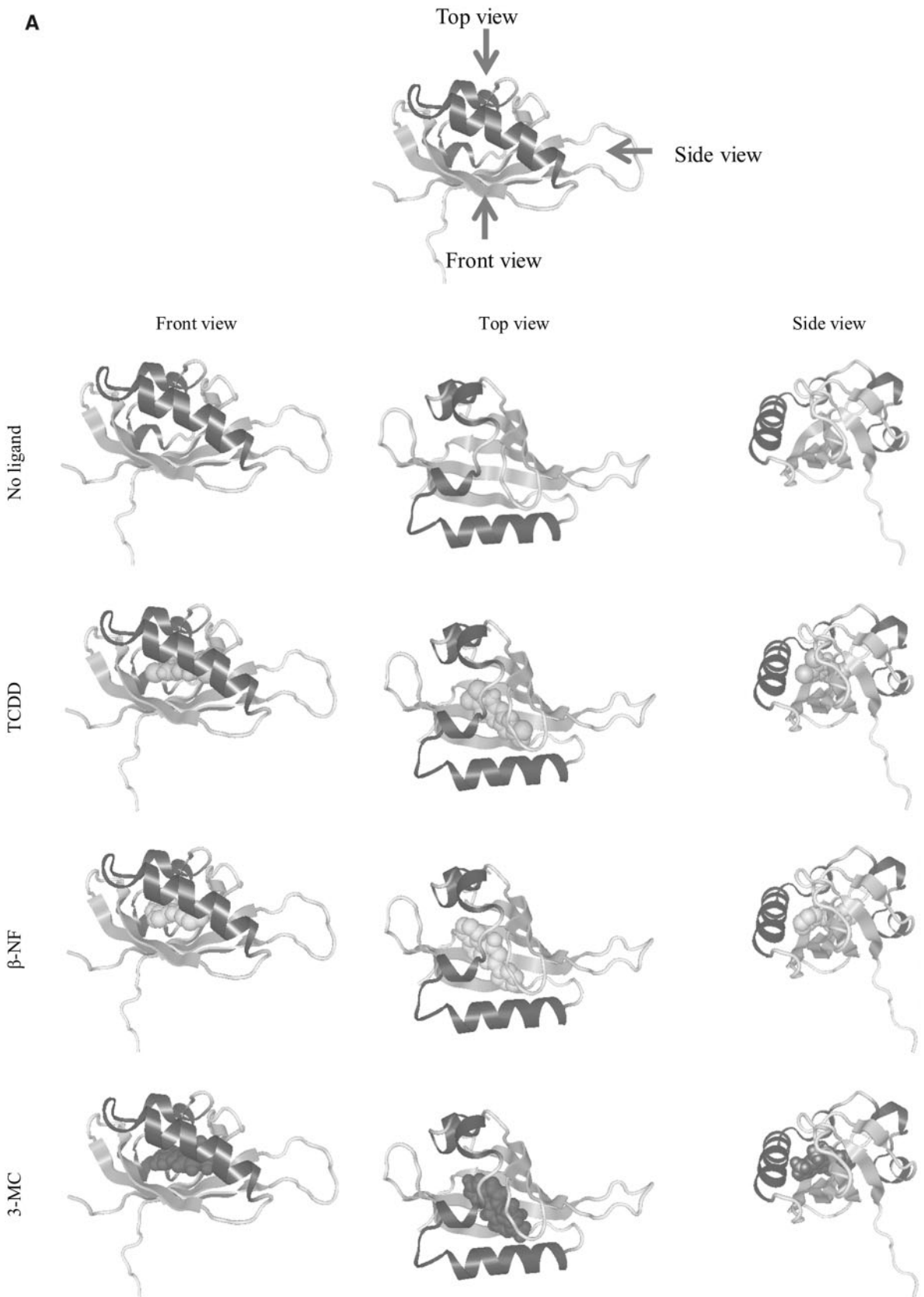

Fig. 4. Molecular modelling. (**A**) Molecular model of HIF-2α with ligand. The molecular models show front view, top view and side view in the absence or presence of the ligand (TCDD, β-NF, 3-MC). (**B**) Secondary structure prediction of AhR PASB domain. The prediction was performed with 272–342 amino acids of AhR using Predict Protein. (**C**) AhR ligand compounds. The structure of the compound was obtained from ChEBI (TCDD; ChEBI ID: 28119, β-NF; ChEBI ID: 77013, 3-MC; ChEBI ID: 34342).

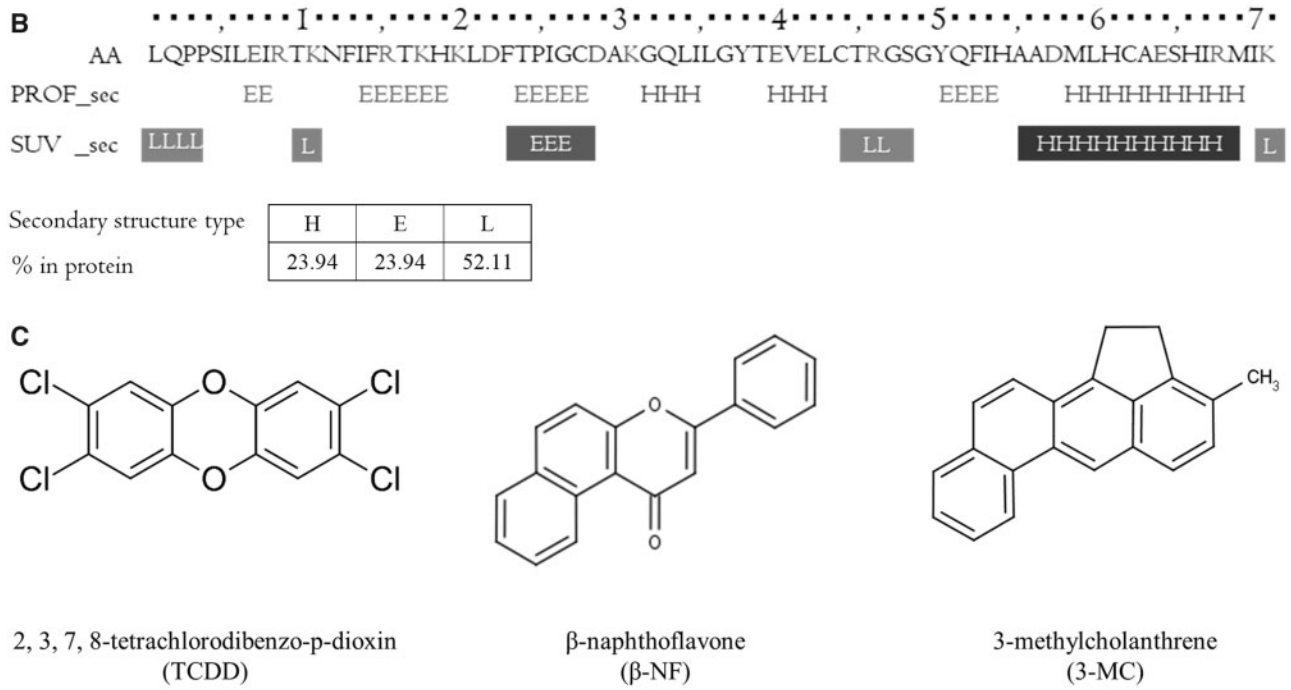

Fig. 4. Continued

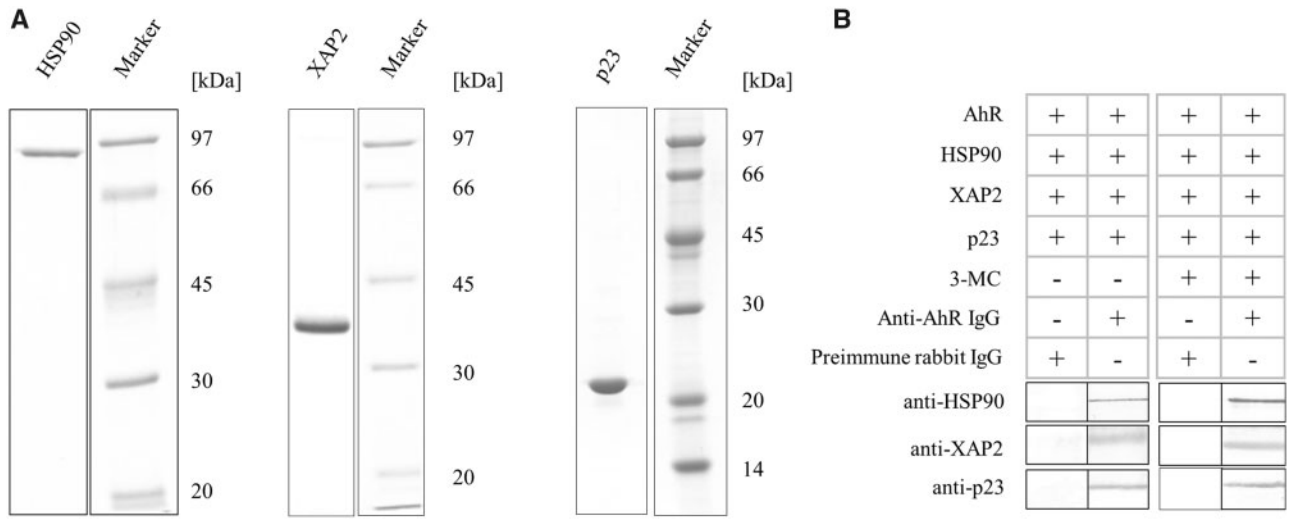

Fig. 5. Analysis of AhR-chaperone complex. (**A**) HSP90, XAP2 and p23 were purified as described under Materials and Methods section. The purified proteins were analysed by SDS-PAGE (11% or 13% gel). (**B**) Analysis of AhR-chaperone complex were performed using anti-AhR antibody in the presence or absence of 3-MC. The immune-precipitated samples were analysed by SDS-PAGE followed by anti-HSP90, anti-XAP2 and antip23 antibodies.

detect the conformational changes of AhR in the presence or absence of ligand.

We predicted the ligand-binding mechanism of AhR using docking simulation software. Since the precise three-dimensional structure of the PAS-B domain of AhR has not been reported, the PAS-B domain of HIF-2α, which is known to be very similar to the PAS-B domain of AhR, was used as a template. The PAS-B domain of HIF-2α possesses two α-helix, five βsheets, and random coil. On the contrary, human PAS-B domain possesses three α-helix, four β-sheets and random structure in the results of PredictProtein. Actually, the PAS-B domains of AhR and HIF-2a appear to be nearly identical. The ligands of TCDD, 3-MC and β-NF bind well to PAS-B domain and each docking score was very high. Each ligand essentially binds to β-sheets of PAS-B domain. The structural changes of AhR occur when ligand binds to β-sheet of PAS-B domain. The conformational changes of AhR in the presence or absence of ligands were investigated using CD spectrum. When a ligand was present, the β-sheet decreased and the α-helix and random structure increased. Secondary structure analysis of full-length AhR is the first report. Generally, the amino

Table II. Docking score of each compounds to AhR

	Docking score
TCDD	−2.540
β-NF	−2.590
3-MC	−2.970
Reserpine	4.250
Methotrexate	2.850

acid M, E, K, A and L is known as an amino acids suitable for α-helix. In the PAS-B domain of human AhR (Fig. 4B), 1L, 7L, 8E, 11K, 18K, 20K, 56A and 57A, these amino acids in the region that does not form an α-helix may be expected to form an α-helix structure after ligand binding. Recently, Schulte *et al.* reported that the crystal structure of the AhR-Arnt core complex bound to its target DNA using human AhR encoding amino acid residues 23-273 (*28*). They presented that the crystal structure of an AhR-Arnt transcription factor complex containing the bHLH and PAS-A domains bound to a 12mer double-stranded DNA (dsDNA). Thus, the XRE binding mechanism of the nuclear AhR-Arnt complex has been elucidated.

The AhR was bound to the HSP90, XAP2 and p23 both in the presence or absence of the ligand. The data were the same as using the AhR PAS or AhR bHLH domain (*20–22*). The purified full-length AhR in the present study possesses a ligand-binding ability and makes a complex with the molecular chaperones. Thus, the purified full-length AhR using the *E. coli* expression system was native form. The purification method can be easily expressed and purified in a laboratory using a common *E. coli* expression system. Many applications are expected, such as a three-dimensional structural analysis of the full-length AhR and search for new ligands of the AhR. We are now investigating the novel non-toxic ligands.

Supplementary Data

Supplementary Data are available at *JB* Online.

Conflict of Interest

None declared.

References

1. Kwapiszewska, G., Johansen, A.K.Z., Gomez-Arroyo, J., and Voelkel, N.F. (2019) Role of the aryl hydrocarbon receptor/ARNT/cytochrome P450 system in pulmonary vascular diseases. *Circ. Res.* **125**, 356–366
2. Bock, K.W. (2019) Aryl hydrocarbon receptor (AHR): from selected human target genes and crosstalk with transcription factors to multiple AHR functions. *Biochem. Pharmacol.* **168**, 65–70
3. McGuire, J., Coumailleau, P., Whitelaw, M.L., Gustafsson, J.A., and Poellinger, L. (1996) The basic helix-loop-helix/PAS factor Sim is associated with hsp90. Implications for regulation by interaction with partner factors. *J. Biol. Chem.* **270**, 31353–31357
4. Antonsson, C., Arulampalam, V., Whitelaw, M.L., Pettersson, S., and Poellinger, L. (1995) Constitutive function of the basic helix-loop-helix/PAS factor Arnt. Regulation of target promoters via the E box motif. *J. Biol. Chem.* **270**, 13968–13972
5. Wu, D., Potluri, N., Kim, Y., and Rastinejad, F. (2013) Structure and dimerization properties of the aryl hydrocarbon receptor PAS-A domain. *Mol. Cell. Biol.* **33**, 4346–4356
6. Feng, S., Cao, Z., and Wang, X. (2013) Role of aryl hydrocarbon receptor in cancer. *Biochim. Biophys. Acta* **1836**, 197–210
7. Jain, S., Dolwick, K.M., Schmidt, J.V. and Bradfield, C.A. (1994) Potent transactivation domains of the Ah receptor and the Ah receptor nuclear translocator map to their carboxyl termini. *J. Biol. Chem.* **269**, 31518–31523
8. Mimura, J. and Fujii-Kuriyama, Y. (2003) Functional role of AhR in the expression of toxic effects by TCDD. *Biochim. Biophys. Acta* **1619**, 263–268
9. Meyer, B.K., Pray-Grant, M.G., Vanden Heuvel, J.P., and Perdew, G.H. (1998) Hepatitis B virus X-associated protein 2 is a subunit of the unliganded aryl hydrocarbon receptor core complex and exhibits transcriptional enhancer activity. *Mol. Cell. Biol.* **18**, 978–988
10. Nebert, D.W. and Gonzalez, F.J. (1987) P450 genes: structure, evolution, and regulation. *Annu. Rev. Biochem.* **56**, 945–993
11. Kazlauskas, A., Poellinger, L., and Pongratz, I. (1999) Evidence that the co-chaperone p23 regulates ligand responsiveness of the dioxin (aryl hydrocarbon) receptor. *J. Biol. Chem.* **274**, 13519–13524
12. Schopf, F.H., Biebl, M.M., and Buchner, J. (2017) The HSP90 chaperone machinery. *Nat. Rev. Mol. Cell Biol.* **18**, 345–360
13. Sahasrabudhe, P., Rohrberg, J., Biebl, M.M., Rutz, D.A., and Buchner, J. (2017) The plasticity of the Hsp90 co-chaperone system. *Mol. Cell* **67**, 947–961
14. Nair, S.C., Toran, E.J., Rimerman, R.A., Hjermstad, S., Smithgall, T.E., and Smith, D.F. (1996) A pathway of multi-chaperone interactions common to diverse regulatory proteins: estrogen receptor, Fes tyrosine kinase, heat shock transcription factor Hsf1, and the aryl hydrocarbon receptor. *Cell Stress Chaperones* **1**, 237–250
15. Perdew, G.H. (1988) Association of the Ah receptor with the 90-kDa heat shock protein. *J. Biol. Chem.* **263**, 13802–13805
16. Tsuji, N., Fukuda, K., Nagata, Y., Okada, H., Haga, A., Hatakeyama, S., Yoshida, S., Okamoto, T., Hosaka, M., Sekine, K., Ohtaka, K., Yamamoto, S., Otaka, M., Grave, E., and Itoh, H. (2014) The activation mechanism of the aryl hydrocarbon receptor (AhR) by molecular chaperone HSP90. *FEBS Open Bio* **4**, 796–803
17. Kudo, I., Hosaka, M., Haga, A., Tsuji, N., Nagata, Y., Okada, H., Fukuda, K., Kakizaki, Y., Okamoto, T., Grave, E., and Itoh, H. (2018) The regulation mechanisms of AhR by molecular chaperone complex. *J. Biochem.* **163**, 223–232
18. Sasaki-Kudo, H., Kudo, I., Kakizaki, Y., Hosaka, M., Ikeda, S., Uemura, S., Grave, E., Togashi, S., Sugawara, T., Shimizu, G., and Itoh, H. (2018) Cisplatin inhibits AhR activation. *AJMB* **08**, 69–82
19. Murray, I.A., Patterson, A.D., and Perdew, G.H. (2014) Aryl hydrocarbon receptor ligands in cancer: friend and foe. *Nat. Rev. Cancer.* **14**, 801–814
20. Beischlag, T.V., Luis Morales, J., Hollingshead, B.D., and Perdew, G.H. (2008) The aryl hydrocarbon receptor complex and the control of gene expression. *Crit. Rev. Eukaryot. Gene Expr.* **18**, 207–250

21. Shinkyo, R., Sakaki, T., Ohta, M., and Inouye, K. (2003) Metabolic pathways of dioxin by CYP1A1: species difference between rat and human CYP1A subfamily in the metabolism of dioxins. *Arch Biochem. Biophys*. **409**, 180–187
22. Chan, W.K., Chu, R.Y., Jain, S., Reddy, J.K., and Bradfield, C.A. (1994) *Baculovirus* expression of the Ah receptor and Ah receptor nuclear translocator - evidence for additional dioxin-responsive element-binding species and factors required for signaling. *J. Biol. Chem*. **269**, 26464–26471
23. Fan, M.Q., Bell, A.R., Bell, D.R., Clode, S., Fernandes, A., Foster, P.M., Fry, J.R., Jiang, T., Loizou, G., MacNicoll, A., Miller, B.G., Rose, M., Shaikh-Omar, O., Tran, L., and White, S. (2009) Recombinant expression of aryl hydrocarbon receptor for quantitative ligand-binding analysis. *Anal. Biochem*. **384**, 279–287
24. Key, J., Scheuermann, T.H., Anderson, P.C., Daggett, V., and Gardner, K.H. (2009) Principles of ligand binding within a completely buried cavity in HIF2alpha PAS-B. *J. Am. Chem. Soc*. **131**, 17647–17654
25. Semenza, G.L. (2004) Hydroxylation of HIF-1: oxygen sensing at the molecular level. *Physiology (Bethesda)* **19**, 176–182
26. Wang, G.L., Jiang, B.H., Rue, E.A., and Semenza, G.L. (1995) Hypoxia-inducible factor 1 is a basic-helix-loop-helix-PAS heterodimer regulated by cellular O_2 tension. *Proc. Natl. Acad. Sci. USA* **92**, 5510–5514
27. Motto, I., Bordogna, A., Soshilov, A.A., Denison, M.S., and Bonati, L. (2011) New aryl hydrocarbon receptor homology model targeted to improve docking reliability. *J. Chem. Inf. Model*. **51**, 2868–2881
28. Schulte, K.W., Green, E., Wilz, A., Platten, M., and Daumke, O. (2017) Structural basis for aryl hydrocarbon receptor-mediated gene activation. *Structure* **25**, 1025–1033